# Experimental Evaluation Method of Asphaltene Deposition Inhibitor's Efficacity at Atmospheric Pressure Using a Fully Immersed Quartz Crystal Resonator, Centrifugation, and Optical Microscopy Techniques

Jawad El Ghazouani, Mohamed Saidoun, Frédéric Tort, Jean-Luc Daridon

# Experimental evaluation method of asphaltene deposition inhibitor's efficacity at atmospheric pressure using a fully immersed Quartz Crystal Resonator, centrifugation and optical microscopy techniques

Jawad El ghazouani[1,2], Mohamed Saidoun[3], Frédéric Tort[4], Jean-Luc Daridon[1*]

[1] Universite de Pau et des Pays de l'Adour, E2S UPPA, CNRS, TotalEnergies, Laboratoire des Fluides Complexes et Leurs Réservoirs, 64000 Pau, France

[2] TotalEnergies, PERL, Pôle Economique 2, BP 47 – RD 817, 64170 Lacq, France

[3] TotalEnergies, CSTJF, Avenue Larribau, 64018 Pau Cedex, France

[4] TotalEnergies, Additives & Fuels Solutions, 69700 Givors, France

Corresponding author

*Jean-Luc Daridon – Email : jean-luc.daridon@univ-pau.fr

KEYWORDS: Asphaltenes, Quartz Cristal Resonator, Centrifugation, Inhibitors, Oil, Destabilization, Deposition.

ABSTRACT

The objective of this paper is to propose a multi-scale method to evaluate the effect of additives on the destabilization and deposition of asphaltenes under conditions of non-diluted crude oil samples. This study shows results of probing asphaltene deposition in presence of a chemical additive using a quartz crystal resonator fully immersed in a dead oil while n-heptane is continuously added. The results obtained show that destabilization is slightly delayed and deposited amount is significantly decreased at concentrations above 3000 ppm of asphaltene deposition inhibitors. The amount of deposited asphaltenes decreases while the inhibitor concentration is increased. In addition, the effect of the chemical is further studied by centrifugation technique to evaluate the concentration of unstable asphaltenes aggregates and the kinetic of aggregation is investigated under optical microscopy observation. Results support the results obtained by quartz crystal resonator and to rule on the evolution of the size/shape of the aggregates.

## 1. INTRODUCTION

Asphaltenes are compounds that have attracted a lot of attention in the oil industry, particularly because of the problems they cause during oil extraction, production and transportation[1]. Naturally occurring in crude oil in the form of suspending nanoaggregates[2] their destabilization is initiated by the effect of oil composition, pressure or temperature variations, followed by an aggregation process. Aggregates containing unstable asphaltene molecules, identified as the source of deposits[3], have a complex chemical structure and follow a complex destabilization mechanisms that involve multi-scale aggregation phenomena from few nanometer to hundreds of micrometers[4].

Asphaltenes are the heaviest and most polar fraction of crude oils. They contains heteroatoms (N,O,S) and heavy metals such as nickel and vanadium[5], which undeniably have an effect on the polarity of asphaltenes and can influence their solubility[6]. Asphaltene molecules contains both polynuclear aromatic core with 4−10 aromatic rings and peripheral aliphatic chains with lengths ranging from 3 to 7 carbon[7].

Numerous techniques have been used to characterize the size and shape of nanoaggregates such as centrifugation[8,9], static light scattering[10], direct-current conductivity[9,11,12], nuclear magnetic resonance (NMR)[13,14], small angle X-ray scattering and neutron scattering (SAXS/SANS)[15,10,16]. These studies have converged towards an organization of polydisperse asphaltene nanoaggregates described as a stack, with an average diameter of 1-2 nm[17], composed of 5 to 9 asphaltenes molecules [18,19,20] created by the $\pi - \pi$ interaction of the aromatic cores and limited by the steric repulsion generated by the peripheral alkyl chains.

A second level of aggregation was observed at higher asphaltene concentrations in toluene described as clusters that consist of less than 12 nanoaggregates and have an average diameter of 5-10 nm[21]. The growth of self-associated asphaltene is limited to the nanoscale in good solvents, leaving them in suspension subject to Brownian motion and to hydrodynamic forces. Further flocculation of clusters is synonym to a commencing destabilization of asphaltenes.

One of the most used solutions to prevent asphaltene deposits on pipeline is to perform continuous or batch injection of chemicals. Their selection is usually performed through laboratory tests to measure their capacity to disperse unstable asphaltenes from crude oils under diluted conditions. There are many methods to measure the dispersing capacity of additives such as Asphaltene Dispersion Test (ADT)[22,23], turbidity test[24,25], ambient pressure near-infrared (NIR) spectroscopy test[26] or centrifugation test[27,28]. The ADT and turbidity tests are performed with diluted crude oils (1-5% volume of crude oil to n-heptane) under static conditions, as opposed to undiluted and flowing oil in industrial conditions. Some other tests are focused on the deposition of unstable asphaltenes like the coupon deposition test[29], electrodeposition test[30], packed bed apparatus[31], capillary test[32] or Quartz Crystal Resonator (QCR)[33,34]. Using piezoelectric properties of quartz, QCR disk sensors allow to evaluate mass deposition on its surfaces[35] in the nanometer range. For this reason, it is also commonly referred to as a QCM (quartz crystal microbalance). However, its applications are not restricted to micro weighting as quartz sensors are sensitive to any change in its surrounding fluid when it is in contact with a fluid[36] or fully immersed in a liquid[37]. Therefore, it appeared to be particularly well suited to probe asphaltene destabilization by sensing both asphaltene mass deposition and bulk property changes[38].

The main objective of this work is to propose a multi-scale set of laboratory tests for an efficient selection of chemical additives for asphaltene deposition reduction. For this purpose, a dead oil supplied by TotalEnergies was studied in the presence or not of a commercial asphaltene deposition inhibitors provided by TotalEnergies Additives & Fuels Solutions. A quartz crystal disk fully immersed in the oil was used to probe asphaltene deposition during n-$C_7$ titration and the inhibition of deposition in the presence of additive was evaluated at the nanoscale. In addition, a centrifugation technique was used to evaluate the effect of the inhibitor on aggregation. Finally, detection time of the appearance of aggregates larger than 500 nm on microscopy and optical microscope equipped with SWIR (Short Wave InfraRed) camera allows to complete the results obtained by quartz crystal resonator.

## 2. MATERIALS AND METHODS

### 2.1 Chemicals

The study was carried out with a dead oil, called oil X, provided by *TotalEnergies* from a field located in West Africa and already put in production. The oil was free from contamination of water, solid particles, production additives or drilling fluids. Standard properties as well as SARA analysis of the dead oil are summarized in Table 1. To conduct this analysis, a sample of dead oil was obtained directly from the bottom tank and flashed in a cold trap. The dead oil was then topped at 323 K and 20 mbar to remove light ends (C15-). The residue was diluted in dichloromethane at a concentration of 15 mg/ml, and an Iatroscan instrument was used to measure saturates, aromatics, and polar fractions (resin + asphaltenes). Saturates were eluted

using n-heptane, while aromatics were eluted using a solvent composed of 25 vol% dichloromethane and 75 vol% n-heptane. The content of asphaltenes was determined by precipitation, using n-pentane as an antisolvent with a weight/volume ratio of 1:40. Before each experiment, the oil was previously heated at 60°C which is above the wax appearance temperature (WAT) of the crude when the oil sample is taken. The commercial asphaltene deposition inhibitor used in this study is from *TotalEnergies Additives & Fuels Solutions*, named here additive A for confidential reasons and his properties are summarized in Table 2. It consists in an alkylphenol resin modified by an alkyl polyamine. This polymer was diluted in Solvarex 150 type of aromatic solvent at a concentration of 42.5% by mass of the active ingredient. In this manuscript, the level of ppm is defined as the ratio of volume concentration of the mother solution (diluted active matter) in the studied mixtures. The experiments were conducted by titration in which the precipitation was induced by the continuous addition of n-heptane at 99+% purity supplied by Sigma Aldrich until the desired concentration of n-heptane was achieved. The concentration of additive in the mixture is kept constant throughout the entire respective experiments (additive initially present in crude oil and in titrant) to avoid dilution effect as titration progresses.

Table 1. Properties of crude oil X

| Property | Value | Technique/Apparatus |
|---|---|---|
| Average Mw (g/mol) | 232 | |
| Density (kg/m$^3$) @ 60°C | 871 | Viscometer Stabinger SVM 3000 – ASTM D7042 |
| Viscosity (mPa.s) @ 60°C | 12,5 | Viscometer Stabinger SVM 3000 – ASTM D7042 |
| Refractive index @ 60 °C | 1.4967 | Mettler Toledo RM40 |

| | | |
|---|---|---|
| Saturates (wt%) | 31.9 | |
| Aromatics (wt%) | 46.6 | |
| Resins (wt%) | 21.5 | |
| Asphaltenes (wt%) | 10.7 | |
| ASCI classification[39] | 11 | |
| Wax appearance temperature (°C) | 41 | Polarized Microscopy[40] |

Table 2. Properties of Additive A

| Property | Value | Technique/Apparatus |
|---|---|---|
| Density ($kg/m^3$) @ 15 °C | 930 | Viscometer Stabinger SVM 3000 – ASTM D7042 |
| Refractive Index @ 60 °C | 1.504 | Mettler Toledo RM40 |

## 2.2 Experimental Methods

### 2.2.1 QCR Experiment

The technique considered here to study asphaltene destabilization and deposition using a thickness shear mode acoustic sensor is based on a titration method. The titration system, which was presented previously[41,42,43] is mainly composed of a stirred batch reactor working at varying volume with an inserted injection system. A schematic diagram of the full experimental setup is presented in Figure 1.

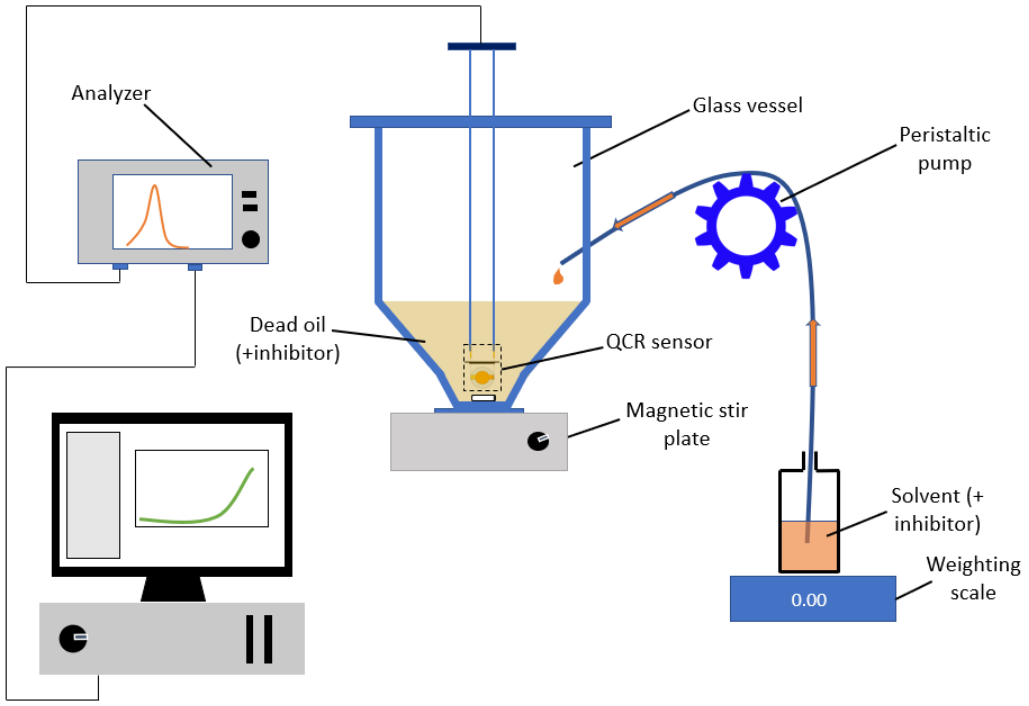


Figure 1. Atmospheric pressure experimental titration QCR set-up.

The temperature-controlled titration cell is a conical glass vessel to achieve an antisolvent injection reaching concentrations between 0 and 90 % in a single run. The antisolvent used in this study is >99% pure grade n-heptane supplied by Sigma Aldrich. Antisolvent is added into the vessel at constant flow rate discharged by a peristaltic pump at constant rate chosen to avoid any local over concentration. The titrant is withdrawn from a container that has been placed on a balance. The mass change in the container is continuously recorded, allowing a direct calculation of the composition of studied system as a function of time. To avoid radial or axial gradients in composition and temperature, the mixture is continuously stirred at a fixed speed of 470 rpm. The stirring speed is maximized while ensuring that the quartz remains fully immersed during the titration. The magnetic stirring bar is 25 mm long and has a diameter of 0.5 mm. Two electrical feedthroughs are used to plug and hold the acoustic sensor immersed in oil during the

entire experiment at the bottom of the cell. The acoustic sensor is a highly polished AT-cut quartz having a fundamental frequency of 3 MHz and a diameter of 13.6 mm with gold electrodes of 6.7 mm in diameter deposited on both sides. QCR sensors are highly sensitive to their thickness, as well as to the thickness of the electrode, and particularly to their surface quality. It is completely impossible to manufacture two sensors with identical properties and therefore with the same resonance properties in air. Thus, it is preferable to use the same QCR for comparative studies. If, unfortunately, the sensor breaks during a lengthy study, it would be necessary to characterize the untreated dead oil using the new sensor before continuing the study. The same quartz disk was reused in this work to allow a reliable comparison of all experiments carried out. It was cleaned between each experiment by consecutive immersions in toluene vials located in an ultrasonic cleaner. Any direct contact of the quartz surface and a solid material is avoided during the washing and drying as well as the storage of the sensor between successive experiments to limit the risk of scratching and consequently changing the resonant properties of the resonator. Cleaning quality is verified by measuring the resonant properties of the unload quartz disk at the same temperature before each new experiment. The cleanliness of quartz surfaces is validated only if the resonance frequency change does not exceed 10Hz / 9 MHz.

The fundamental resonance frequency as well as the geometry of the quartz was selected to allow the sensor to be operational in an extended overtone range (from 3 to 7) in full immersion in viscous oils. A network analyser was used to apply a radio frequency voltage to the quartz sensor and to measure the input port voltage reflection coefficient $S_{11}$ which is used to calculate the conductance of the quartz over the frequency range from fundamental to $7^{th}$ overtone. The resonance frequency $f_n$ of each overtone correspond to the maximum of a conductance peak in

the conductance spectrum. The resonance frequencies are estimated with an uncertainty of 4 Hz whereas the resonance half-band half-width $\Gamma_n$ (related to resonator dissipation) is determined with a maximum error of 5 Hz. The unloaded reference values $f_0$ and $\Gamma_0$ are obtained by applying unload measurements (air) prior to each experiment. Reference frequencies and dissipation are respectively used to calculate the shift in resonant properties caused by fluid immersion $\Delta f_n$ and $\Delta\Gamma_n$.

In case of full immersion within a Newtonian fluid, a simplified model can be used to correlate changes in resonant frequency (eq 1) and half-band half-width (eq 2) of the sensor with the properties of the surrounding system [44,45,41] :

$$\Delta f_n = -n(2c_m\Delta m) - \sqrt{n}\frac{C_m}{\sqrt{\pi f_0}}\sqrt{\rho\eta} \quad (1)$$

$$\Delta\Gamma_n = \sqrt{n}\frac{C_m}{\sqrt{\pi f_0}}\sqrt{\rho\eta}\,(1+R) \quad (2)$$

where $C_m$ is the Sauerbrey's coefficient that depends on the crystal characteristics, $n$ is the overtone number, $f_0$ is the fundamental resonance frequency of the crystal, $\Delta m$ is the theoretical adsorbed or deposited mass on the quartz surface, $\rho\eta$ is the density-viscosity product of the surrounding fluid and $R$ is an empirical correction term for the viscous friction of the fluid on rough surfaces of the sensor. Extension of this simple model to asphaltene systems by considering $\Delta m$ as the sum of surface effect and asphaltene deposition makes it possible to estimate changes in both asphaltene deposited mass (per unit area) and viscosity-density product in the fluid surrounding the sensor.

In this work, each of the studied solutions were prepared as follows with a rigorously identical protocol to compare results with or without asphaltene deposition inhibitors (AI):

i) 25 $cm^3$ of the studied mixture is poured into the cell.

ii) The crude + additive mixture is left under stirring at the working temperature for 1 hour to achieve equilibrium between quartz sensor surface and the surrounding oil.

iii) The heptane is injected at constant mass flow rate of 0.25 g/min.

For the interpretation of recorded data, the shift in resonant frequency and half-band half-width are calculated and plotted as a function of either time or volume fraction of n-heptane in the mixture $\phi_{C7}$ expressed as a function of the volume of each component:

$$\phi_{C7} = \frac{V_{C7}}{V_{C7}+V_{oil}+V_{AI}} \quad (3)$$

The major point of asphaltene destabilization, elsewhere referred to as "onset", is defined as the intersect of the opposed slopes before and after the observed inflexion point of the resonance frequency (Figure 2). At this point, resonant behavior deviates from the simple dilution Kanazawa law. In practice, frequency signal of quartz crystal resonator appeared predominantly affected by mass deposition of asphaltenes, if any, explaining the major change of slope of the frequency[46]. Consequently, the shift in frequency plot was prefeed to estimate the onset. Finally, the change of deposited mass was estimated by plotting $\Delta f_n/\sqrt{n}$ as a function of $\sqrt{n}$ and calculating its slope according to equation 1.

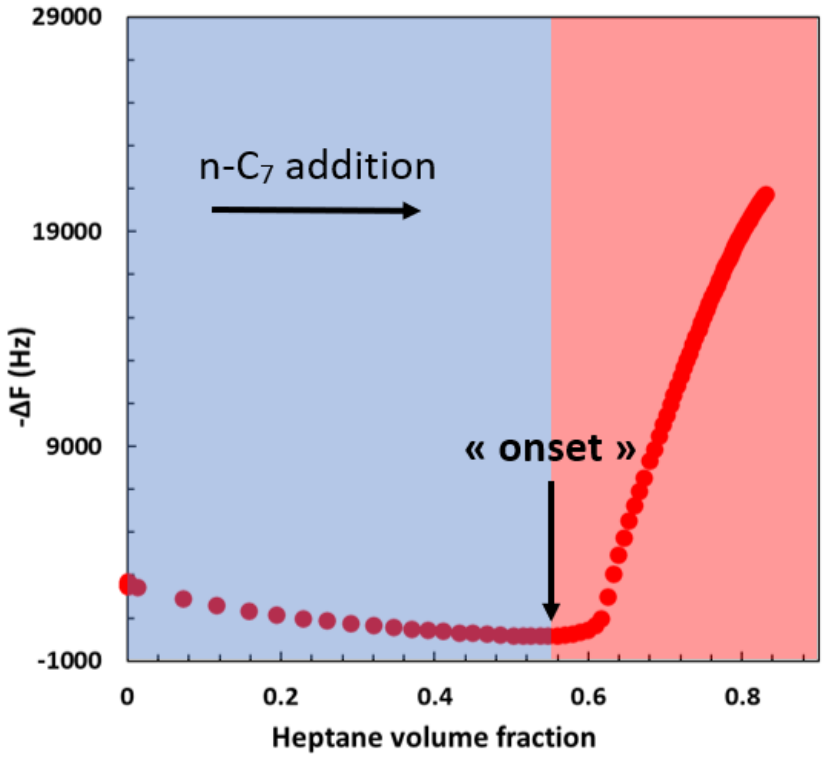


Figure 2. Determination of "onset" from resonance frequency measurements.

### 2.2.2 Centrifugation Experiment

The content of unstable asphaltenes per unit volume of crude oil at specific aging time $C_A(t)$ was measured here by the time-resolved centrifugation method reported by Maqbool et al[47]. The samples were prepared following the same protocol as presented for QCR experiments. Mixtures of non-treated oil and oil + additive A at 3000 ppm (in volume) were prepared with a content in heptane of 51.1% and 51.2% in volume respectively. After their preparation the samples with the desired heptane composition were sealed and maintained under stirring at 470 rpm and 60°C during aging process. Aliquots of 1.5 ml were taken over time and centrifuged with the *Rotina 380R* from *Hettich* at 15,000 rpm. Centrifugation times, was fixed at 14 minutes to reach a

separation efficiency cut-off size of 200 nm. The calculation method used is the one proposed by Saidoun[48].

In this method, the supernatant is drained and recovered centrifuged pellets are collected as "wet" cakes containing unstable asphaltenes and trapped liquid solution. Pellets are washed with heptane several times, re-dispersed and re-centrifuged until the supernatant remains transparent. Finally, the mass of dried cake is used to calculate the concentration of unstable asphaltenes aggregates larger than the cut-off size per unit volume of initial crude oil. The concentration of separated unstable asphaltenes aggregates $C_A(t)$ is plotted as a function of the aging time for different oil-heptane blend systems for the interpretation. $C_A(t)$ is expected to increase with the aging time for a fixed mixture and eventually tends to an equilibrium (plateau region).

### 2.2.3 SWIR microscopy experiment

Because of the darkness of the oil, it is difficult to observe the shape and size of aggregates using a standard microscope with a high magnification. Instead, a short-wave infrared (SWIR) camera coupled to a microscope was used at wavelengths where the absorption of light by heavy hydrocarbons is reduced. A custom optical assembly was used, it was developed around video microscope unit (VMU mitutoyo)[49] paired with a x50 to x100 objectives with a long working distance and correction for infrared wavelengths. A camera using an InGaAs sensor was mounted onto the VMU for measurement in the infrared bandwidth from 0.9 to 1.7 μm. A sample of the oil X + additive A mixture at different additive concentrations was taken at 83 vol% of titrant and placed in a two polished windows cell with a path length of 1mm for immediately observation under a microscope with X50 magnification.

### 2.2.4 Detection Time Experiment

Following the procedure introduced by Maqbool et al.[47], the detection time of unstable asphaltenes in oil-heptane mixtures was measured with and without addition of additive. Solutions were prepared with the same protocol described in earlier sections. When the desired volume fraction of heptane in the oil-heptane mixture was reached, the flask was sealed, and the mixture was kept in this condition at 60°C under constant stirring (at 470 rpm) for the time necessary to achieve the full study. Aliquots of each sample were taken at controlled aging times using a capillary and observed under a microscope with a magnification of x20. The detection time corresponds to the aging time after which asphaltene flocs are first observed and confirmed to further grow by microscopy. The experiment was repeated for multiple volume fractions of antisolvent with and without additive. A plot of the detection time as a function of the volume fraction of heptane was obtained as a result the experiments. This plot is referred to as the detection time curve. It ranges from few minutes for large antisolvent fraction up to a hundred of hours for low antisolvent fraction. The lowest concentrations of antisolvent for which the detection-time is less than 5 minutes is considered as the instantaneous detection condition by microscopy.

### 2.2.5 Turbidity experiment

In addition, absorbance measurements were carried out to compare the results obtain with other techniques. Asphaltenes were precipitated by adding 100 μL of crude oil sample with (or

without) additive to 3 mL of n-heptane in a vial. The mixture was manually homogenized, and the absorbance evolution of the blend was measured as a function of time.

The turbidity measurements were obtained using a *Cary 60 UV-Vis Spectrophotometer* from *Agilent* using a near-infrared light source of 800 nm.

## 3. RESULTS AND DISSCUSION

The role of an asphaltene deposition inhibitor's is to reduce deposit thickness or to delay its build-up period. However, the addition of an additive does not systematically lead to a positive effect for preventing asphaltene deposition. Moreover, Barcenas et al. demonstrated that increasing the amount of additives injected does not always results in a higher interaction with asphaltenes[50]. To evaluate the efficacy of an additive, laboratory tests were conducted to identify the working concentration that shows a positive effect on asphaltene destabilization and on diffusion deposition process trying to replicate driving forces of asphaltene destabilization in industrial operating conditions. The results of these tests were summarized below.

### 3.1 Turbidity experiment

The turbidity test is one of the most common approach used in laboratory for evaluating the effectiveness of additives based on the dispersion efficiency of asphaltenes in presence of chemicals. This method evaluates the ability of an additive to keep destabilized asphaltenes in suspension. The higher the absorbance, the more dispersed the asphaltenes are. The results of absorbance measurements with concentrations ranging from 10 ppm to 3000 ppm (in volume) of additives in oil/n-heptane mixtures are shown in Figure 3. From 100 ppm the absorbance is

maintained at a higher value than for the untreated reference oil. The unstable asphaltene aggregates are therefore maintained in suspension in the presence of the additive over this period of one hour. The effect of the concentration above 300 ppm appears negligible. With this type of technique where the destabilizing precipitant/oil ratios have to be higher than 90% in volume and the medium remains static during the measurement, the question of representativeness with field conditions can be asked. Hence the need to resort to experiments with more realistic destabilizing precipitant/oil ratio conditions and focusing on scales of measures that enable to more clearly discriminate the effectiveness of additives.

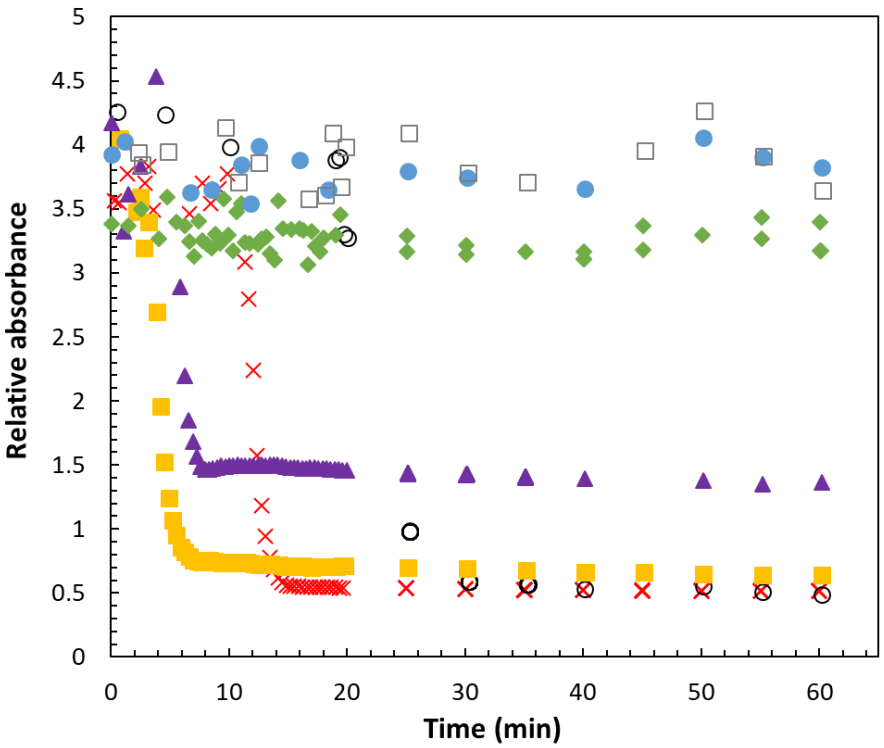


Figure 3. Relative absorbance of Oil X in presence of additive A at different concentrations: (red×) 0ppm, (black ○) 10ppm, (yellow ■) 30ppm, (purple ▲) 100ppm, (green ◆) 300ppm, (blue ●) 1000ppm, (grey □) 3000ppm.

### 3.2 QCR experiment - Additive effect on crude oil: Raw data ($\Delta f$ and $\Delta\Gamma_n$) analysis

Titration experimentations of n-heptane in dead crude oil with an immersed QCR sensor were carried out with various additive dosages and compared with crude oil free of chemical additives. During these experiments both the shift in resonance frequency and changes in bandwidth along various overtones (1 to 7) of the resonating sensor were recorded and analyzed for comparison.

The change in resonance frequency of the third overtone peak measured by the quartz crystal immersed in pure crude oil and in the presence of additive with different contents ranging from 300 to 20 000 ppm (in volume) are shown in Figure 4. It can be noted in this figure that for an addition of 300 ppm of additive, destabilization is shifted to lower heptane composition in comparison to the shift in frequency of free additive crude oil. No change was detected on the destabilization curve beyond the onset. At 1000 ppm no significant effect was observe on the threshold whereas a decrease in the amplitude of the shift in frequency was noted after the onset. From 3000 ppm the destabilization is slightly shifted towards higher compositions and this effect is more marked as the additive concentration is important. For 3000 ppm we observe a shift in destabilization of +2.2 % in volume fraction compared to the reference measurement (pure crude oil) and +8.5% and +11.4% for 10 000 ppm and 20 000 ppm respectively. These results show that more than 1000 ppm of additive A is required to shift the destabilization of asphaltenes to a higher antisolvent composition. In addition, the onset shift is greater as the concentration of additive is increased but appears to reach a plateau value near 20 000 ppm.

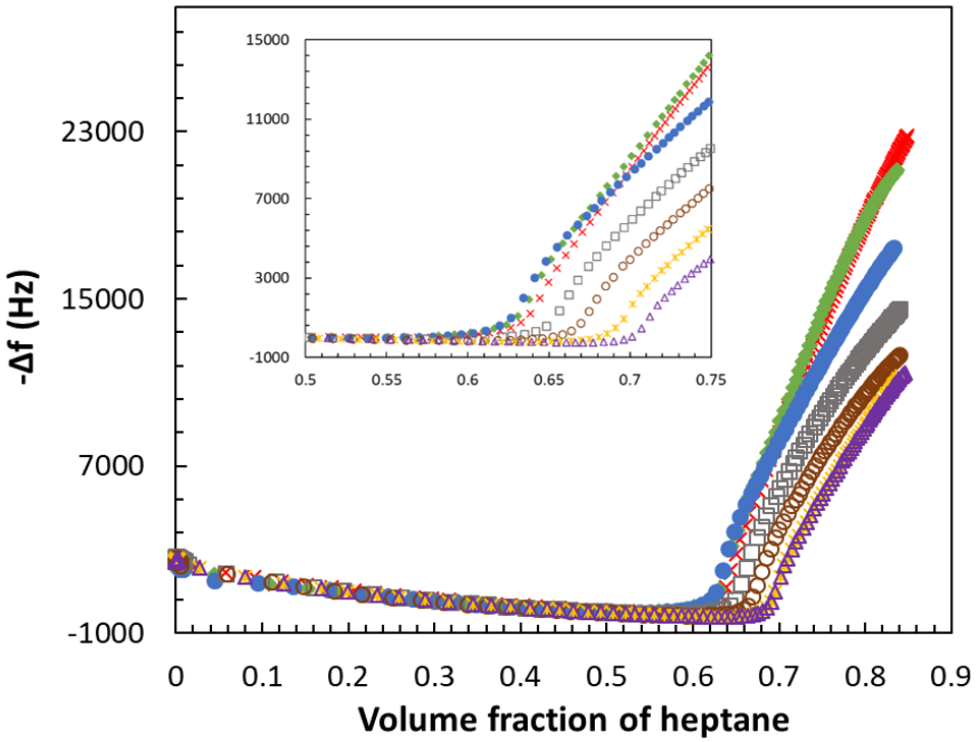


Figure 4. Shift of resonance frequency (3rd harmonic) recorded during experimental titration of crude oil X + additive A at different concentrations as a function of the volume fraction of heptane: (red×) 0ppm, (green ◆) 300ppm, (blue ●) 1000ppm, (grey □) 3000ppm, (brown ○) 5000ppm, (yellow ∗) 10 000ppm, (purple △) 20 000ppm. A zoom of the frequency shift between 0.5 and 0.75 volume fraction of heptane is shown in the inner box.

As for the change in resonance frequency, the shift in the bandwidth was only plotted for the third overtone peak in Figure 5. This figure shows for each concentrations an increase in dissipation with a maximum then a decrease. Daridon et al. demonstrated, using the simple Einstein viscosity equation, that for an oil with a viscosity similar to that of Oil X (10 mPa.s), small changes in $\Delta\Gamma$ can be associated with a change in volume fraction. The sensor is capable of detecting a minimum value equivalent to $1.1 \times 10^{-3}$ for the 3rd harmonic, for a $\Delta\Gamma$ of 5 Hz[46].

For all samples, titration curves first decrease because of the reduction in viscosity caused by the addition of heptane (dominating dilution effect). Then the increase in dissipation is related to the destabilization of the asphaltenes and the growth of asphaltene aggregates suspended around the sensor. The quartz disk therefore detects larger and/or more objects close to its surface. This increase in dissipation is shifted towards higher heptane compositions as the AI concentration is increased. Furthermore, the amplitude of the dissipation peak increases as the additive concentration in solution is increased.

From these measurements and from equation 1 and 2 it is possible to extract the mass deposited on the quartz surface as well as the change in density viscosity product of the fluid in contact with the sensor. The apparent viscosity is calculated according to the following equation:

$$(\rho\eta)_\Gamma = \frac{\pi f_0}{{C_m}^2}\left(\frac{\Delta\Gamma_n}{1+R}\right)^2$$

(4)

Where $\Delta\Gamma_n$ here is $\Delta\Gamma_3$ as a function of the square root of 3 (eq 2). Only the 3rd harmonic was used for several reasons. Firstly, it appears that the first harmonic is particularly affected by intrinsic properties of quartz crystals such as piezoelectric stiffening and edge effects[51], which means that it behaves differently from other harmonics and cannot be used. For the largest harmonics, it has been shown that inharmonic resonances interfere with the main resonance peaks[52]. Finally, the 3rd harmonic has the greatest penetration length of the acoustic wave in the contacting media (eq. 5). The ratio $\frac{\Delta f_\eta}{\Delta f_m}$ is proportional to $\frac{1}{\sqrt{n}}$, which makes it possible to estimate the bulk viscosity-density product from 3rd harmonic peak with less impact from the properties of the deposited layer than with higher harmonics.

$$\eta = \sqrt{\frac{\mu_{liq}}{n\pi f_0 \rho_{liq}}}$$

(5)

The density is calculated using the molar mass/molar volume ratio of the mixture during continuous addition of heptane. Theoretical viscosity change with addition of heptane was calculated using the Grunberg-Nissan type of equation[53] (eq 6) assuming a binary mixture composed of crude oil + heptane.

$$\eta = \exp(x \ln(\eta_{hep}) + (1-x) \ln(\eta_{oil}) + x(1-x)G)$$

(6)

In this expression, the Grunberg-Nissan parameter G was adjusted to match the apparent viscosity measured by QCR before asphaltenes destabilization.

Results in Figure 6 indicate that the aggregation of asphaltenes after heptane addition promotes a slight increase of the viscosity. A shift in the increase in dissipation is observed in presence of additive and it is proportional to the additive concentration.

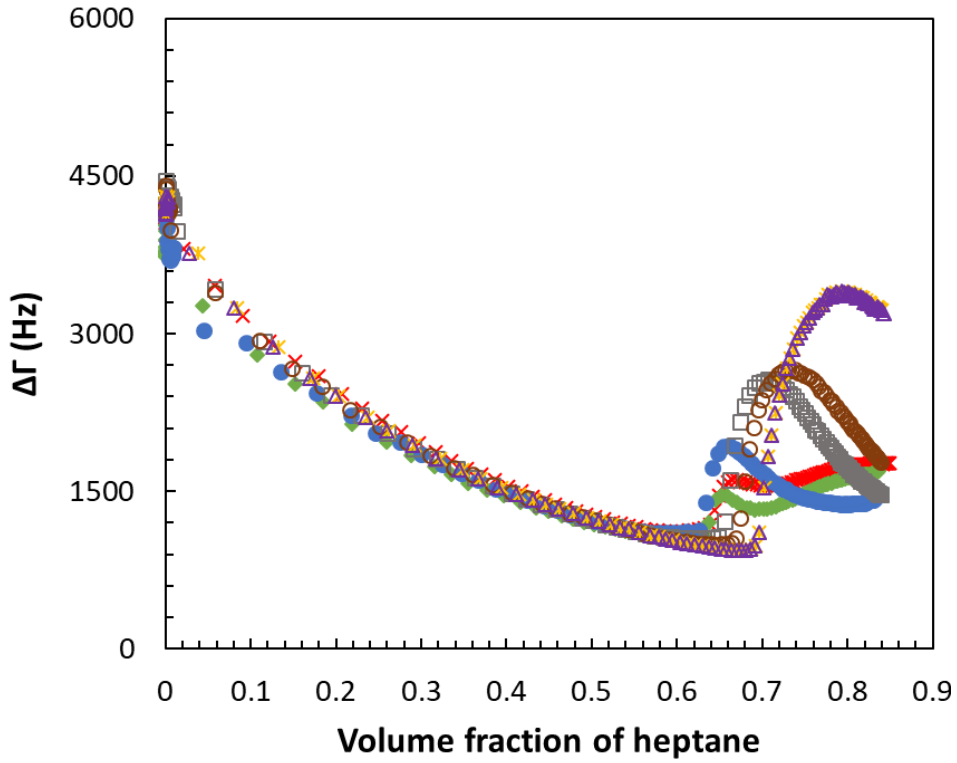


Figure 5. Shift of dissipation (3rd harmonic) recorded during experimental titration of crude oil X + additive A at different concentrations as a function of the volume fraction of heptane: (red×) 0ppm, (green ◆) 300ppm, (blue ●) 1000ppm, (grey □) 3000ppm, (brown ○) 5000ppm, (yellow ∗) 10 000ppm, (purple △) 20 000ppm.

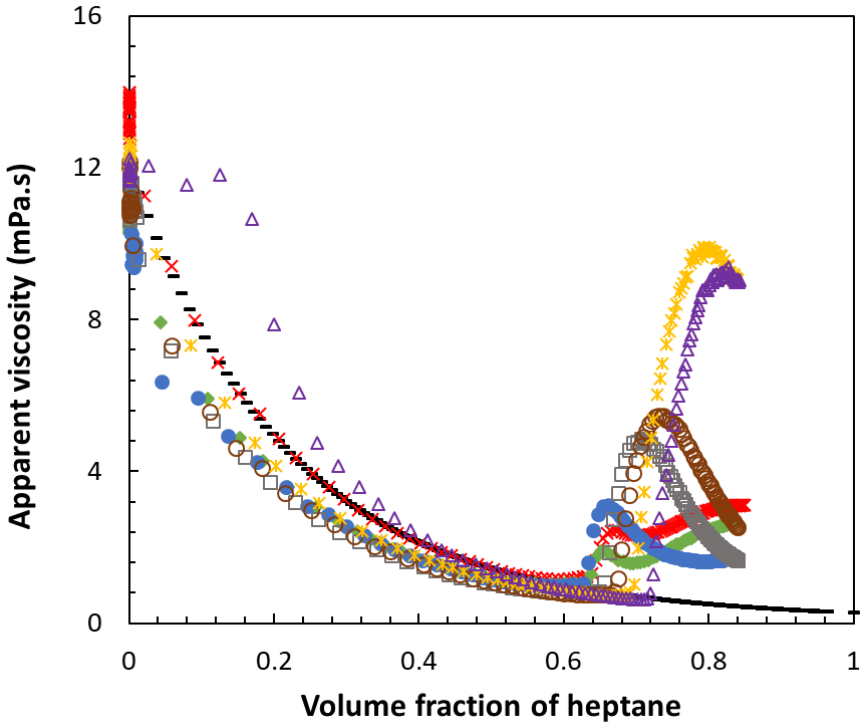


Figure 6. Apparent viscosity of the surrounding fluid calculated during experimental titration of crude oil X + additive A at different concentrations as a function of the volume fraction of heptane: (black -) theorical viscosity, (red×) 0ppm, (green ◆) 300ppm, (blue ●) 1000ppm, (grey □) 3000ppm, (brown ○) 5000ppm, (yellow ∗) 10 000ppm, (purple △) 20 000ppm.

The deposited mass can be evaluated by expressing equation 1 in terms of $\Delta f_n/\sqrt{n}$ as a function $\sqrt{n}$ and by calculating the slope of the obtained straight line[38]. The values obtained by this method during the titration were displayed in Figure 7. Starting from a concentration of 1000 ppm of additive A, a clear decrease of the deposit compared to non-treated oil is shown.

For the purpose to evaluate and compare the positive additive effect on deposition reduction, the deposition inhibition efficiency in the presence of additive A at a volume concentration of 80 vol% was calculated according to the following equation:

$$\text{Deposition inhibition } \% = \left(1 - \frac{Deposited\ mass\ @\ 80\ vol\%\ with\ AI}{Deposited\ mass\ @\ 80\ vol\%\ Pure\ Crude\ Oil}\right) * 100 \quad (7)$$

The results are reported in Table 3. As it can be inferred from this Table 3 very few effects were observed at low concentration of additive (300 ppm). At excessive concentrations of AI (>10 000ppm) the effects seem to tend towards an inhibition efficiency of 90% at a volume composition of 80% in antisolvent. The subsequent working concentration was set at 3000 ppm for further evaluation of the additive because at this concentration the deposition inhibition efficiency is sufficiently clear, and the concentration is not excessive in relation to the real use conditions in the industry.

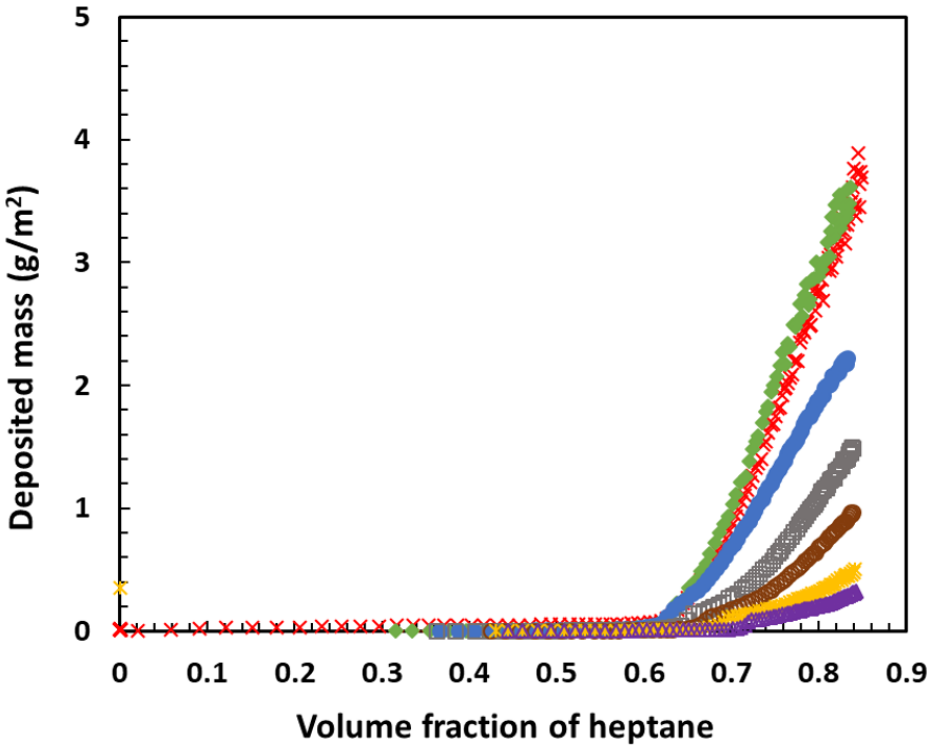


Figure 7. Deposited mass calculated during experimental titration of crude oil X + additive A at different concentrations as a function of the volume fraction of heptane: (red×) 0ppm, (green ◆) 300ppm, (blue ●) 1000ppm, (grey □) 3000ppm, (brown ○) 5000ppm, (yellow ∗) 10 000ppm, (purple △) 20 000ppm.

Table 3. Deposition inhibition efficiency of oil treated by additive A at 80 vol% heptane composition.

| Additive A concentration (ppm) | Deposition inhibition efficiency |
|---|---|
| 300 | -5.91 % |
| 1000 | 32.84 % |
| 3000 | 60.96 % |

| | |
|---|---|
| 5000 | 75.27 % |
| 10,000 | 88.51 % |
| 20,000 | 92.28 % |

### 3.3 Centrifugation experiment

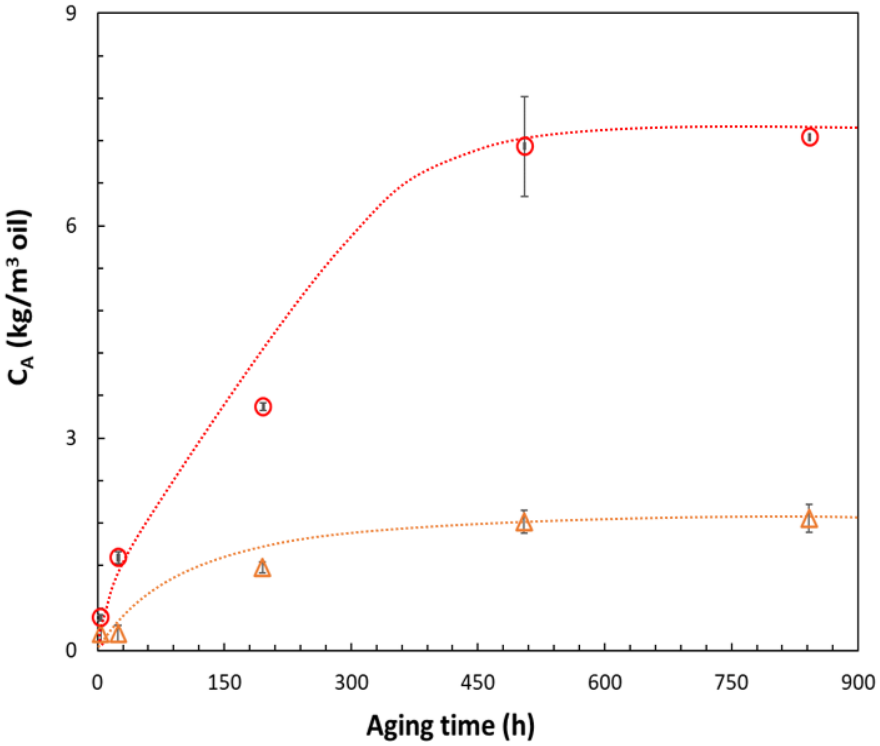


Figure 8. Concentration of unstable asphaltenes larger than 200 nm separated by centrifugation as a function of the aging time of prepared blends of crude Oil X and heptane: (red ○) non-treated Oil X + 51.1 vol% of n-C7, (orange △) Oil X + additive A (3000ppmv) + 51.2 vol% of n-C7. The dotted lines are made to facilitate the reading of the trends.

The concentration of unstable asphaltenes aggregates larger than 200 nm centrifuged per unit of volume of crude oil at specific aging time $C_A(t)$ is represented as function of the aging time of

the crude oil-heptane mixture in Figure 8. The results show that the amount of separable asphaltenes destabilized from oil-heptane mixture is reduced by the presence of additive A. Equilibrium plateau values are reached at aging times higher than 500h; about 1.9 kg/m$^3$ oil in the presence of additive A compared to 7.2 kg/m$^3$ oil for the untreated oil.

### 3.4 SWIR microscopy

The titration tests carried out with the quartz crystal sensor indicated a delayed destabilization of asphaltenes, reduced mass deposition on quartz surfaces, and an increased dissipation of the signal in presence of additive. This increase in dissipation (proportional to an apparent viscosity) can reflect a change in the morphology of the flocs formed far from the onset of destabilization. To observe this change in floc structures in the micrometer range SWIR microscopy observations were performed at the end of the titration. To make these observations comparable, a sample of titrated oil was taken instantaneously after the titration experiment and directly transferred to the glass cell of the microscope. All the samples investigated corresponded to a heptane volume fraction of 0.83. The results are shown in Figure 9. Without additive, the aggregates have a size between 25 and 45 micrometers in diameter and have a globular-like shape in this condition of sampling (Figure 9. A). A clear decrease in aggregate size is observed above 3000 ppm (Figure 9. C, D, E and F) in the same conditions of sampling. From 10 000ppm the size of aggregates does not seem to decrease anymore. Moreover, as the concentration of additive A is increased, the aggregates are less and less spherical and some aggregates with needle shapes are observed.

The reduction of the size of the aggregates observed in presence of chemical additive at this micrometer scale is very likely related to the stabilization of aggregates by amphiphilic properties of additive. Indeed, it was reported in the literature that amphiphiles with their polar

head will react with the active sites of asphaltenes[54,55,56]. Once attached to the asphaltenes, the hydrophobic tail of the amphiphiles will generate a steric repulsion and thus limit the size of the asphaltene aggregates[55,57].

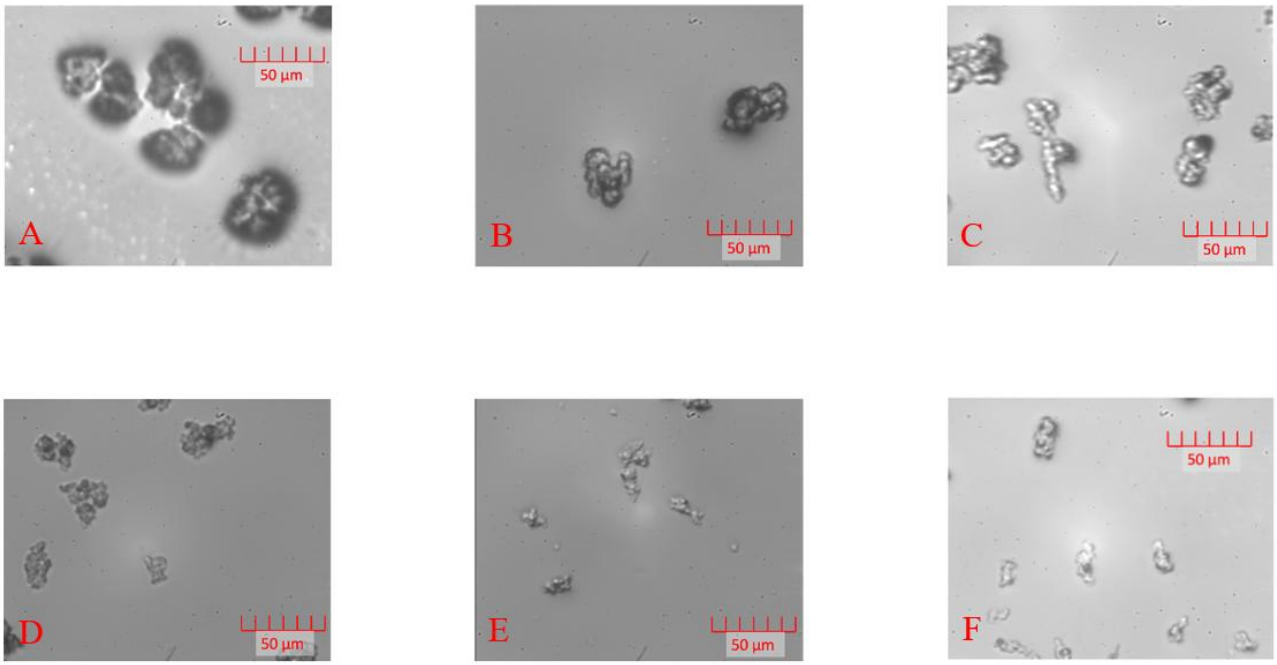


Figure 9. SWIR camera capture at X50 magnification of crude Oil X + additive A samples at 83 vol% heptane: (A) 0ppm, (B) 1000ppm, (C) 3000ppm, (D) 5000ppm, (E) 10 000ppm, F 20 000ppm.

## 3.5 Detection Time experiment

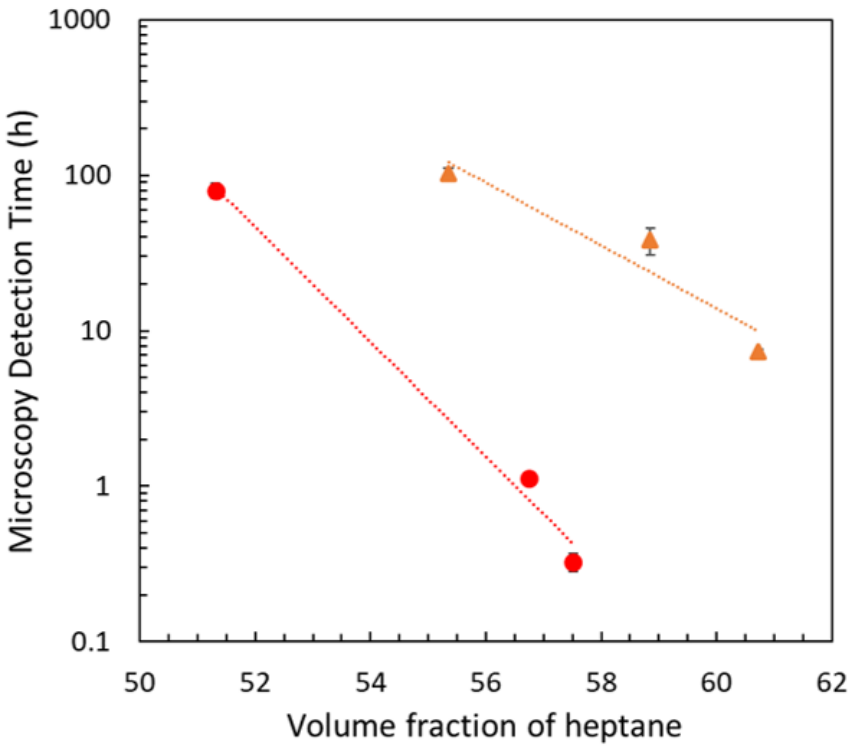


Figure 10 : Necessary aging time to detect particles by visual microscopy observations as function of the volume fraction of heptane in heptane-oil blends: (red ●) non-treated Oil X, (orange ▲) Oil X + additive A at 3000ppmv.

The detection time curves are shown in Figure 10 for Oil X as pure reference crude oil and the same oil treated by additive A at 3000 ppm in volume. The instantaneous microscopy detection of asphaltene aggregates in Oil X + heptane was observed at ~58 vol% of heptane and ~61 vol% for oil treated with additive A. This result is consistent with observed minimum shift in frequency (-Δf) of the resonating immersed sensor; i.e. at 55.2 vol% of heptane in Oil X and 57.4 vol% of heptane treated oil X with 3000 ppm of additive A (refer to Figure 4). This way, the larger sensitivity of the quartz resonator compared to microscopy is also verified, as expected. Indeed, the microscope observations describe the appearance of aggregates larger than 500 nm while the quartz allows the detection of nanometer level. Nevertheless, both techniques show a

delay of the same order of magnitude in the observation destabilization of asphaltenes in the presence of additive at nanoscale and microscale.

The presence of additive A in crude oil delays the observation of asphaltene aggregates by 1 to 2 orders of magnitudes at heptane fractions inferior to 60 vol% in oil X. Results suggest that Additive A stabilizes asphaltene aggregates by keeping them in suspension.

## 4. CONCLUSION

Raw and processed data obtained from the QCR sensor were used to compare asphaltenes destabilization and deposition during a titration of pure crude oil and crude oil with additive. It allowed to evaluate the efficacy of an AI through measurements in the nanometer scale. Results show that additive A shifted the destabilization towards higher antisolvent compositions with an increased effect as the concentration of additive in solution is increased. From 1000 ppm onwards a decrease of the deposit with an increase of the AI concentration was observed. This effect seems to be limited between 10,000 ppm and 20,000 ppm, and it can be assumed that there is a threshold above which the increase in AI concentration no longer has a significant impact on deposition. Excessive AI increase did not negatively impact the amount of deposition and no AI self-assembly effect was observed. Moreover, the results obtained in QCR were supported by the results obtained in centrifugation where a clear decrease in concentration of destabilized particles larger than 200 nm was observed in the presence of additive. The effect of the additive on the aggregation kinetics was also highlighted by the detection time measurements with a delay in appearance of unstable asphaltenes aggregates larger than 500 nm.

These observations are consistent with the results obtained by the QCR and the effect of additives on the response of quartz to dissipation. Indeed, it has been described previously that the increase in dissipation is linked to an increase in the viscosity of the crude-heptane mixture, which is itself linked to the appearance of flocs in the environment close to the quartz disk.

Absorbance measurements showed the capacity of the additive to maintain these particles in suspension and thus to limit their size.

Increasing the concentration of additive A showed a shift in the increase of viscosity compared to the pure crude oil which is consistent with the shift in the appearance of aggregates under the microscope and shows the effect of the additive in delaying the destabilization towards higher antisolvent compositions.

This research aims at providing solutions to the industry, confronted to problems related to the accumulation of asphaltene deposits on the walls of pipelines but also to the accumulation of sedimented particles under static conditions. Hence, results of this manuscript show that evaluating effectiveness of an additive in laboratories must study the deposition as well as the aggregation kinetics. In addition, the study of viscosity is interesting especially for the evaluation of the effectiveness of a “flow improver” additive.

Immersed resonating sensors and centrifugation (or microscopy) methods are showed to be complementary techniques for the screening of asphaltene inhibitors.

AUTHOR INFORMATION

**Corresponding Author**

*Jean-Luc Daridon − Universite de Pau et des Pays de l'Adour, E2S UPPA, CNRS, TotalEnergies, Laboratoire des Fluides Complexes et Leurs Réservoirs, 64000 Pau, France; orcid.org/0000-0002-0522-0075.

E-mail : jean-luc.daridon@univ-pau.fr.

**Notes**

The authors declare no competing financial interest.

ACKNOWLEDGMENTS

We would like to acknowledge the following people who have contributed to this project and and for the fruitful discussions: Nelson Acevedo, Nicolas Passade-Boupat and Moussa Kane. The authors would also like to thank TotalEnergies for providing the oil sample and TotalEnergies Additives & Fuels Solutions for supplying the chemical additive.

REFERENCES

(1) Adams, J. J. Asphaltene Adsorption, a Literature Review. *Energy Fuels* **2014**, *28* (5), 2831–2856.

(2) Mullins, O. C.; Sabbah, H.; Eyssautier, J.; Pomerantz, A. E.; Barré, L.; Andrews, A. B.; Ruiz-Morales, Y.; Mostowfi, F.; McFarlane, R.; Goual, L.; Lepkowicz, R.; Cooper, T.; Orbulescu, J.; Leblanc, R. M.; Edwards, J.; Zare, R. N. Advances in Asphaltene Science and the Yen–Mullins Model. *Energy Fuels* **2012**, *26* (7), 3986–4003.

(3) Katz, D. L.; Beu, K. E. Nature of Asphaltic Substances. *Ind. Eng. Chem.* **1945**, *37* (2), 195–200.

(4) Hoepfner, M. P.; Vilas Bôas Fávero, C.; Haji-Akbari, N.; Fogler, H. S. The Fractal Aggregation of Asphaltenes. *Langmuir* **2013**, *29* (28), 8799–8808.

(5) Ancheyta, J.; Centeno, G.; Trejo, F.; Marroquín, G. Changes in Asphaltene Properties during Hydrotreating of Heavy Crudes. *Energy Fuels* **2003**, *17* (5), 1233–1238.

(6) Kaminski, T. J.; Fogler, H. S.; Wolf, N.; Wattana, P.; Mairal, A. Classification of Asphaltenes via Fractionation and the Effect of Heteroatom Content on Dissolution Kinetics. *Energy Fuels* **2000**, *14* (1), 25–30.

(7) Groenzin, H.; Mullins, O. C. Asphaltene Molecular Size and Weight by Time-Resolved Fluorescence Depolarization. In *Asphaltenes, Heavy Oils, and Petroleomics*; Mullins, O. C., Sheu, E. Y., Hammami, A., Marshall, A. G., Eds.; Springer: New York, NY, 2007; pp 17–62.

(8) Mostowfi, F.; Indo, K.; Mullins, O. C.; McFarlane, R. Asphaltene Nanoaggregates Studied by Centrifugation. *Energy Fuels* **2009**, *23* (3), 1194–1200.

(9) Goual, L.; Sedghi, M.; Zeng, H.; Mostowfi, F.; McFarlane, R.; Mullins, O. C. On the Formation and Properties of Asphaltene Nanoaggregates and Clusters by DC-Conductivity and Centrifugation. *Fuel* **2011**, *90* (7), 2480–2490.

(10) Eyssautier, J.; Frot, D.; Barré, L. Structure and Dynamic Properties of Colloidal Asphaltene Aggregates. *Langmuir* **2012**, *28* (33), 11997–12004.

(11) Goual, L. Impedance Spectroscopy of Petroleum Fluids at Low Frequency. *Energy Fuels* **2009**, *23* (4), 2090–2094.

(12) Zeng, H.; Song, Y.-Q.; Johnson, D. L.; Mullins, O. C. Critical Nanoaggregate Concentration of Asphaltenes by Direct-Current (DC) Electrical Conductivity. *Energy Fuels* **2009**, *23* (3), 1201–1208.

(13) Sheremata, J. M.; Gray, M. R.; Dettman, H. D.; McCaffrey, W. C. Quantitative Molecular Representation and Sequential Optimization of Athabasca Asphaltenes. *Energy Fuels* **2004**, *18* (5), 1377–1384.

(14) Lisitza, N. V.; Freed, D. E.; Sen, P. N.; Song, Y.-Q. Study of Asphaltene Nanoaggregation by Nuclear Magnetic Resonance (NMR). *Energy Fuels* **2009**, *23* (3), 1189–1193.

(15) Sheu, E. Y. Self-Association of Asphaltenes. In *Structures and Dynamics of Asphaltenes*; Mullins, O. C., Sheu, E. Y., Eds.; Springer US: Boston, MA, 1998; pp 115–144.

(16) Hoepfner, M. P.; Fogler, H. S. Multiscale Scattering Investigations of Asphaltene Cluster Breakup, Nanoaggregate Dissociation, and Molecular Ordering. *Langmuir* **2013**, *29* (49), 15423–15432.

(17) Mullins, O. C.; Sabbah, H.; Eyssautier, J.; Pomerantz, A. E.; Barré, L.; Andrews, A. B.; Ruiz-Morales, Y.; Mostowfi, F.; McFarlane, R.; Goual, L.; Lepkowicz, R.; Cooper, T.;

Orbulescu, J.; Leblanc, R. M.; Edwards, J.; Zare, R. N. Advances in Asphaltene Science and the Yen–Mullins Model. *Energy Fuels* **2012**, *26* (7), 3986–4003.

(18) Schneider, M. H.; Andrews, A. B.; Mitra-Kirtley, S.; Mullins, O. C. Asphaltene Molecular Size by Fluorescence Correlation Spectroscopy. *Energy Fuels* **2007**, *21* (5), 2875–2882.

(19) Tanaka, R.; Sato, E.; Hunt, J. E.; Winans, R. E.; Sato, S.; Takanohashi, T. Characterization of Asphaltene Aggregates Using X-Ray Diffraction and Small-Angle X-Ray Scattering. *Energy Fuels* **2004**, *18* (4), 1118–1125.

(20) Wu, Q.; Pomerantz, A. E.; Mullins, O. C.; Zare, R. N. Laser-Based Mass Spectrometric Determination of Aggregation Numbers for Petroleum- and Coal-Derived Asphaltenes. *Energy Fuels* **2014**, *28* (1), 475–482.

(21) Simon, S.; Jestin, J.; Palermo, T.; Barré, L. Relation between Solution and Interfacial Properties of Asphaltene Aggregates. *Energy Fuels* **2009**, *23* (1), 306–313.

(22) Juyal, P.; Ho, V.; Yen, A.; Allenson, S. J. Reversibility of Asphaltene Flocculation with Chemicals. *Energy Fuels* **2012**, *26* (5), 2631–2640.

(23) Hashmi, S. M.; Quintiliano, L. A.; Firoozabadi, A. Polymeric Dispersants Delay Sedimentation in Colloidal Asphaltene Suspensions. *Langmuir* **2010**, *26* (11), 8021–8029.

(24) Shadman, M. M.; Vafaie-Sefti, M.; Ahmadi, S.; Assaf, M. A.; Veisi, S. Effect of Dispersants on the Kinetics of Asphaltene Settling Using Turbidity Measurement Method. *Petroleum Science and Technology* **2016**, *34* (14), 1233–1239.

(25) Kraiwattanawong, K.; Fogler, H. S.; Gharfeh, S. G.; Singh, P.; Thomason, W. H.; Chavadej, S. Effect of Asphaltene Dispersants on Aggregate Size Distribution and Growth. *Energy & Fuels* **2009**, 23 (3), 1575-1582.

(26) Melendez-Alvarez, A. A.; Garcia-Bermudes, M.; Tavakkoli, M.; Doherty, R. H.; Meng, S.; Abdallah, D. S.; Vargas, F. M. On the Evaluation of the Performance of Asphaltene Dispersants. *Fuel* **2016**, *179*, 210–220.

(27) Jennings, D. W.; Chao, K.-P.; Kim, J. Asphaltene Inhibitor Testing: Comparison between a High Pressure Live-Fluid Deposition and Ambient Pressure Dead-Oil Asphaltene Stability Method. Proceedings of the Offshore Technology Conference; Houston, TX, April 30−May 3, 2018.

(28) Balestrin, L. B. da S.; Francisco, R. D.; Bertran, C. A.; Cardoso, M. B.; Loh, W. Direct Assessment of Inhibitor and Solvent Effects on the Deposition Mechanism of Asphaltenes in a Brazilian Crude Oil. *Energy Fuels* **2019**, *33* (6), 4748–4757.

(29) Bae, J.; Fouchard, D.; Garner, S.; Macias, J. Advantages of Applying a Multifaceted Approach to Asphaltene Inhibitor Selection. Proceedings of the Offshore Technology Conference; Houston, TX, May 2−5, 2016.

(30) Mena-Cervantes, V. Y.; Hernández-Altamirano, R.; Buenrostro-González, E.; Beltrán, H. I.; Zamudio-Rivera, L. S. Tin and Silicon Phthalocyanines Molecularly Engineered as Traceable Stabilizers of Asphaltenes. *Energy Fuels* **2011**, *25* (1), 224–231.

(31) Vilas Bôas Fávero, C.; Hanpan, A.; Phichphimok, P.; Binabdullah, K.; Fogler, H. S. Mechanistic Investigation of Asphaltene Deposition. *Energy Fuels* **2016**, *30* (11), 8915–8921.

(32) Vilas Bôas Fávero, C.; Maqbool, T.; Hoepfner, M.; Haji-Akbari, N.; Fogler, H. S. Revisiting the Flocculation Kinetics of Destabilized Asphaltenes. *Advances in Colloid and Interface Science* **2017**, *244*, 267–280.

(33) Enayat, S.; Tavakkoli, M.; Yen, A.; Misra, S.; Vargas, F. M. Review of the Current Laboratory Methods To Select Asphaltene Inhibitors. *Energy Fuels* **2020**, *34* (12), 15488–15501.

(34) Ekholm, P.; Blomberg, E.; Claesson, P.; Auflem, I. H.; Sjöblom, J.; Kornfeldt, A. A Quartz Crystal Microbalance Study of the Adsorption of Asphaltenes and Resins onto a Hydrophilic Surface. *Journal of Colloid and Interface Science* **2002**, *247* (2), 342–350.

(35) G, S. Use of the Vibrating Quartz for Thin Film Weighing and Microweighing. *Z. Phys.* **1959**, *155*, 206.

(36) Keiji Kanazawa, K.; Gordon, J. G. The Oscillation Frequency of a Quartz Resonator in Contact with Liquid. *Analytica Chimica Acta* **1985**, *175*, 99–105.

(37) Cassiède, M.; Mejia, A.; Radji, S.; Carrier, H.; Daridon, J.-L.; Saidoun, M.; Tort, F. Evaluation of the Influence of a Chemical Inhibitor on Asphaltene Destabilization and Deposition Mechanisms under Atmospheric and Oil Production Conditions Using QCM and AFM Techniques. *Energy Fuels* **2021**, *35* (21), 17551–17565.

(38) Daridon, J. L.; Cassiède, M.; Nasri, D.; Pauly, J.; Carrier, H. Probing Asphaltene Flocculation by a Quartz Crystal Resonator. *Energy Fuels* **2013**, *27* (8), 4639–4647.

(39) Passade-Boupat, N., Zhou, H., Rondon-Gonzalez, M., "Asphaltene precipitation from crude oils: how to predict it and to anticipate treatment?", SPE-164184.

(40) Daridon, J.-L.; Pauly, J.; Milhet, M. High Pressure Solid-Liquid Phase Equilibria in Synthetic Waxes. *Physical Chemistry Chemical Physics* **2002**, *4* (18), 4458.

(41) Daridon, J. L.; Cassiède, M.; Nasri, D.; Pauly, J.; Carrier, H. Probing Asphaltene Flocculation by a Quartz Crystal Resonator. *Energy Fuels* **2013**, *27* (8), 4639–4647.

(42) Saidoun, M.; Palermo, T.; Passade-Boupat, N.; Gingras, J.-P.; Carrier, H.; Daridon, J.-L. Revisiting Asphaltenes Instability Predictions by Probing Destabiliztion Using a Fully Immersed Quartz Crystal Resonator. *Fuel* **2019**, *251*, 523–533.

(43) Acevedo, N.; Moulian, R.; Chacón-Patiño, M. L.; Mejia, A.; Radji, S.; Daridon, J.-L.; Barrère-Mangote, C.; Giusti, P.; Rodgers, R. P.; Piscitelli, V.; Castillo, J.; Carrier, H.; Bouyssiere, B. Understanding Asphaltene Fraction Behavior through Combined Quartz Crystal Resonator Sensor, FT-ICR MS, GPC ICP HR-MS, and AFM Characterization. Part I: Extrography Fractionations. *Energy Fuels* **2020**, *34* (11), 13903–13915.

(44) Johannsmann, D. Viscoelastic Analysis of Organic Thin Films on Quartz Resonators. *Macromolecular Chemistry and Physics* **1999**, *200* (3), 501–516.

(45) Lucklum, R.; Behling, C.; Hauptmann, P. Role of Mass Accumulation and Viscoelastic Film Properties for the Response of Acoustic-Wave-Based Chemical Sensors. *Anal. Chem.* **1999**, *71* (13), 2488–2496.

(46) Daridon, J.-L.; Carrier, H. Measurement of Phase Changes in Live Crude Oil Using an Acoustic Wave Sensor: Asphaltene Instability Envelope. *Energy Fuels* **2017**, *31* (9), 9255–9267.

(47) Maqbool, T.; Balgoa, A. T.; Fogler, H. S. Revisiting Asphaltene Precipitation from Crude Oils: A Case of Neglected Kinetic Effects. *Energy Fuels* **2009**, *23* (7), 3681–3686.

(48) Saidoun, M. Investigations into Asphaltenes Destabilization, Aggregation and Deposition. 239.

(49) Daridon, J.-L.; Lin, C.-W.; Carrier, H.; Pauly, J.; Fleming, F. P. Combined Investigations of Fluid Phase Equilibria and Fluid–Solid Phase Equilibria in Complex CO2–Crude Oil Systems under High Pressure. *J. Chem. Eng. Data* **2020**, *65* (7), 3357–3372.

(50) Barcenas, M.; Orea, P.; Buenrostro-González, E.; Zamudio-Rivera, L. S.; Duda, Y. Study of Medium Effect on Asphaltene Agglomeration Inhibitor Efficiency. *Energy Fuels* **2008**, *22* (3), 1917–1922.

(51) Cassiède, M.; Paillol, J. H.; Pauly, J.; Daridon, J.-L. Electrical Behaviour of AT-Cut Quartz Crystal Resonators as a Function of Overtone Number. *Sensors and Actuators A: Physical* **2010**, *159* (2), 174–183.

(52) Cassiède, M.; Daridon, J.-L.; Paillol, J. H.; Pauly, J. Characterization of the Behaviour of a Quartz Crystal Resonator Fully Immersed in a Newtonian Liquid by Impedance Analysis. *Sensors and Actuators A: Physical* **2011**, *167* (2), 317–326.

(53) Grunberg, L.; Nissan, A. H. Mixture Law for Viscosity. *Nature* **1949**, *164* (4175), 799–800.

(54) González, G.; Middea, A. Peptization of Asphaltene by Various Oil Soluble Amphiphiles. *Colloids and Surfaces* **1991**, *52*, 207–217.

(55) Chang, C.-L.; Fogler, H. S. Stabilization of Asphaltenes in Aliphatic Solvents Using Alkylbenzene-Derived Amphiphiles. 1. Effect of the Chemical Structure of Amphiphiles on Asphaltene Stabilization. *Langmuir* **1994**, *10* (6), 1749–1757.

(56) Chang, C.-L.; Fogler, H. S. Stabilization of Asphaltenes in Aliphatic Solvents Using Alkylbenzene-Derived Amphiphiles. 2. Study of the Asphaltene-Amphiphile Interactions and Structures Using Fourier Transform Infrared Spectroscopy and Small-Angle X-Ray Scattering Techniques. *Langmuir* **1994**, *10* (6), 1758-1766.

(57) León, O.; Rogel, E.; Urbina, A.; Andújar, A.; Lucas, A. Study of the Adsorption of Alkyl Benzene-Derived Amphiphiles on Asphaltene Particles. *Langmuir* **1999**, *15* (22), 7653–7657.

TOC graphic

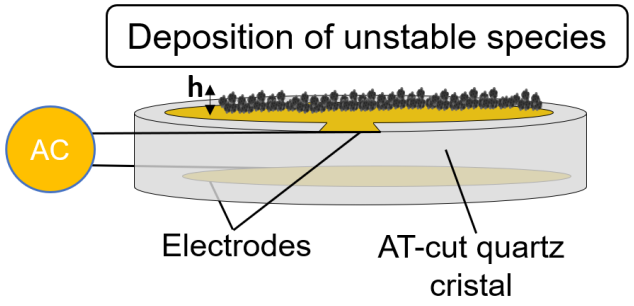
Deposition of unstable species
h
AC
Electrodes
AT-cut quartz
cristal